RSC Pharmaceutics

ROYAL SOCIETY OF CHEMISTRY

PAPER

View Article Online
View Journal | View Issue

Cite this: *RSC Pharm.*, 2024, **1**, 296

Thermodynamic and spectroscopic evaluation of the eutectic mixture of myristic acid and the local anaesthetics, bupivacaine and ropivacaine

Priyanka Agarwal, *[a] Darren Svirskis[a] and Michél K. Nieuwoudt[b,c,d,e]

Local anaesthetics provide an opioid-sparing alternative for pain management; however, their short-lived analgesic effect necessitates repeat or sustained drug delivery to the target site. Improving drug loading and enhancing physical stability is a challenge when formulating sustained release devices. Here, myristic acid's interaction with bupivacaine and ropivacaine was studied to evaluate whether eutectic formation between these drugs and myristic acid can similarly influence drug crystallization and increase drug loading in poly ethylene-*co*-vinyl acetate (EVA). Binary mixtures of ropivacaine and bupivacaine with myristic acid were thermodynamically evaluated by differential scanning calorimetry. Fourier transfer infrared (FTIR) spectra of bupivacaine or ropivacaine and myristic acid binary mixtures at different ratios were obtained and synchronous and asynchronous two-dimensional correlation spectroscopy (2DCOS) maps analysed. Stabilizing effects were observed visually by preparing EVA films containing each drug with and without myristic acid. Thermodynamic and spectroscopic studies suggested that both bupivacaine and ropivacaine form a eutectic with myristic acid at the molar ratio of 2 : 3 and 1 : 3, respectively. 2DCOS FTIR analysis revealed hydrogen bonding between the carbonyl and hydroxyl groups of myristic acid and amide carbonyl group of bupivacaine and ropivacaine, respectively, when myristic acid was present in excess. Furthermore, myristic acid transiently stabilized both bupivacaine and ropivacaine in EVA matrices, but crystallization was evident by the 6-month timepoint. Myristic acid forms a eutectic with both bupivacaine and ropivacaine due to hydrogen bonding interaction. Eutectic formation inhibits crystallization and stabilizes bupivacaine and ropivacaine in EVA matrices, for 1 month, however crystallization of both local anaesthetics was evident after 6-months.

Received 20th December 2023,
Accepted 12th March 2024

DOI: 10.1039/d3pm00082f

rsc.li/RSCPharma

Introduction

In recent years, the need for opioid sparing analgesics in post-operative pain management has become glaringly obvious with local anesthetics (LAs) emerging as safe and efficient alternatives.[1–3] The amide type LAs, bupivacaine and ropivacaine, prevent depolarization of sodium channels by binding to their intracellular domains and inhibiting neural transmission of pain signals.[4,5] Bupivacaine is most frequently used for continuous epidural and other regional analgesia techniques due to its long duration of action and a favorable ratio of sensory to motor neural block.[6,7] However, due to its propensity for cardiac and central nervous system toxicity in some patients, the application of ropivacaine, which has comparable efficacy,[8,9] but with a greater degree of motor sensory differentiation and potentially improved safety profile,[10,11] is now gaining prominence.

A significant limitation of both bupivacaine and ropivacaine, however, is their rapid systemic absorption and short lived analgesic effect[8,9] necessitating continuous infusion, which increasing the risk of post-surgical complications.[12–14] Consequently, significant research has been directed towards the development of dosage regimens and drug delivery systems that prolong analgesia by reducing systemic clearance and/or enabling sustained release of LAs at the target site.[15] Several liposomal or micro- and nanoparticulate systems have been evaluated for sustained release of bupivacaine and ropivacaine.[16–18] However, poor stability, short shelf life and the inability to retrieve such colloidal injections in the event of dose dumping and toxicity have limited their clinical appli-

[a]*School of Pharmacy, Faculty of Medical and Health Science, The University of Auckland, New Zealand. E-mail: p.agarwal@auckland.ac.nz*
[b]*School of Chemical Sciences, The University of Auckland, New Zealand*
[c]*The Photon Factory, The University of Auckland, New Zealand*
[d]*The Dodd-Walls Centre for Photonic and Quantum Technologies, New Zealand*
[e]*The MacDiarmid Institute for Advanced Materials and Nanotechnology, New Zealand*

cation. Implantable polymer systems for sustained release of LAs can help in overcoming these limitations and facilitate better control over drug pharmacokinetics.

Recently, the suitability of a poly(ethylene-*co*-vinyl acetate) (EVA) based implantable device for extended lidocaine delivery for 3–7 days was demonstrated in an ovine model.[19] Myristic acid was used to stabilize lidocaine up to a concentration of 20% w/w in the EVA matrix. Thermodynamic and spectroscopic evaluation suggested that hydrogen bonding interactions between lidocaine and myristic acid resulted in eutectic formation and inhibited association between adjacent lidocaine molecules and prevented drug crystallization.[20] To extend the application of this approach, the current study aims to evaluate whether bupivacaine and ropivacaine, which have similar functional groups as lidocaine but are structurally distinct due to the presence of a piperidine ring, also interact with myristic acid in a similar fashion. Thermodynamic interactions of bupivacaine and ropivacaine with myristic acid were evaluated by differential scanning calorimetry (DSC) while the mechanism of the interaction was studied using Fourier-transform infrared spectroscopy (FTIR). Two-dimensional correlation spectroscopy (2DCOS) analysis of the FTIR spectra was performed to decipher the correlations between different spectral features of bupivacaine or ropivacaine interactions with myristic acid. Furthermore, the stability of bupivacaine and ropivacaine in EVA matrices with and without myristic was evaluated to ascertain whether myristic acid's stabilizing effect also extended to these drugs.

Experimental

Materials

Bupivacaine was purchased from Cayman Chemical Company, Ann Arbor, MI, USA, while ropivacaine was purchased from AK Scientific, Union City, CA, USA. EVA (Ateva 3325 comprising 33% vinyl acetate) was provided by Celanese, Edmonton, Alberta, Canada. Dichloromethane was purchased from Merck, Darmstadt, Germany and potassium bromide for IR spectroscopy was purchased from Honeywell Fluka™ Seelze, Germany.

Thermal analysis of local anaesthetic and myristic acid binary mixtures

The thermal properties of myristic acid, bupivacaine and ropivacaine, as well as their binary mixtures containing varying molar ratios of each LA and myristic acid, were evaluated by differential scanning calorimetry (DSC; Q2000, TA instruments, New Castle, DE, USA) using Pyris Manager software (version 10.1) with nitrogen (20 mL min^{-1}) as the purge gas.

Binary mixtures of bupivacaine–myristic acid and ropivacaine–myristic acid were prepared by triturating bupivacaine or ropivacaine with myristic acid in a mortar and heating the mixture in an oven maintained at 60 °C for 15 min. The heated mixture typically had a semi-solid or liquid consistency and was agitated well with a pestle before cooling under laminar flow. The mixtures were then weighed and sealed in aluminum pans. The DSC cycle involved a heating ramp at a rate of 2 °C min^{-1} from 0 to 140 °C and 0 to 160 °C for bupivacaine–myristic and ropivacaine–myristic acid binary mixtures, respectively. The resulting melting points for each LA–myristic acid binary mixture were plotted graphically as a function of percentage molar ratio of LA to construct phase diagrams. The molar ratio at which a single melting endotherm of the liquid eutectic was obtained was termed the eutectic ratio with the melting temperature being the eutectic temperature.[21] All experiments were performed in triplicate.

Spectroscopic evaluation of local anaesthetic and myristic acid binary mixtures

The interaction of binary mixtures of each LA with myristic acid at multiple ratios was evaluated using FTIR spectroscopy in transmission mode. In contrast to ATR (attenuated total reflectance) mode, which measures only up to 4–6 μm beneath the surface of around 1 mm^2 area, transmission mode allows measurement of a larger volume of sample and is thus more accurate for quantitative measurement. The spectroscopic software program OMNIC (V4.1, Thermo Fisher Scientific, Waltham, USA) was used for processing the spectra. Samples were prepared by triturating 2–3 mg of the binary mixtures with 200 mg of potassium bromide (KBr) and pressing into pellets. FTIR spectra were obtained in transmission mode using a Bruker Tensor 37 FTIR spectrometer equipped with OPUS 6.5 software (Ettlingen, Germany). For each sample, 32 scans were obtained between 4000 cm^{-1} and 400 cm^{-1} at the resolution of 4 cm^{-1} using a 6 mm aperture. A blank KBr pellet was also prepared and collected as the background for each set of sample spectra recorded.

Preparation of EVA films containing local anaesthetic and myristic acid

EVA films weighing 0.5 g and containing either bupivacaine (3% w/w, 6% w/w or 9% w/w) or ropivacaine (3% w/w, 6% w/w or 9% w/w) alone or in combination with myristic acid (myristic acid concentration being equivalent to the eutectic ratio with each LA, as determined by DSC) were prepared by adapting a previously described solvent casting method.[22] Briefly, appropriate quantities of the EVA, bupivacaine or ropivacaine and myristic acid were dissolved in 15 mL of dichloromethane by shaking the samples at 100 rpm in a water bath maintained at 37 °C for 2 hours. The clear solution obtained was cooled before being poured in pre-cooled glass Petri dishes. The films were dried under laminar flow for at least 72 hours after which, they were carefully peeled and stored at room temperature. All films were visually observed for crystallization over 6 months.

Results and discussion

Thermal analysis of binary mixtures

Thermal properties of the drugs and their binary mixtures with myristic acid were studied by DSC to investigate the inter-

action between them and to predict the molar ratio at which such an interaction is optimum. For pure bupivacaine, ropivacaine and myristic acid, an endothermic melting peak was observed on the first heating ramp at 103.8 ± 1.1 °C, 146.9 ± 0.7 °C and 54.2 ± 0.3 °C, while exothermic recrystallization peak was evident during the subsequent cooling ramp at 96.8 ± 3.2 °C, 124 ± 1.9 °C, 50.9 ± 0.2 °C, respectively. For myristic acid and ropivacaine, the endothermic melting point and its enthalpy during both the heating cycles was the same, suggesting complete recrystallization. However, for pure bupivacaine, additional thermal events were observed during the second heating ramp with a change in enthalpy of the endothermic peak at 106 °C, possibly due to recrystallisation of bupivacaine into multiple stable and metastable polymorphic forms, as described previously.[21]

The binary mixtures of bupivacaine and ropivacaine were prepared for DSC by heating and homogenization in a mortar since the melting point of both drugs is higher than the flash point of myristic acid.[23] For binary mixtures of both drugs, two melting endotherms were observed at all ratios, a solidus melting point close to the eutectic temperature and a liquidus melting point attributed to the melting of excess solid in the eutectic compound.[24] However, at one specific ratio, the solidus and liquidus peak merged to give a single sharp endothermic peak at a temperature significantly lower than the melting points of the drugs and myristic acid individually (Fig. 1), suggesting that a eutectic may have formed.[25,26] This ratio was the eutectic point (E), and its melting point was termed as the eutectic temperature. Eutectic points of bupivacaine–myristic acid and ropivacaine–myristic acid binary mixtures were observed at the molar ratio of 2 : 3 (30.4 ± 1.0 °C) and 1 : 3 (40.2 ± 0.8 °C), respectively.

FTIR spectroscopic evaluation of the binary mixtures

FTIR spectra of the binary mixtures of each drug with myristic acid were measured at the eutectic ratio (*i.e.* 2 : 3 bupivacaine : myristic acid and 1 : 3 ropivacaine : myristic acid) since this composition was hypothetically most favourable for an interaction between the LA drug and myristic acid. In addition, spectra of the binary mixtures prepared at half and twice the eutectic ratio (*i.e.* 1 : 3 and 4 : 3 bupivacaine : myristic acid and 1 : 1.5 and 1 : 6 ropivacaine : myristic acid) were measured to study the interaction under non-ideal conditions. As a first indication of whether bonding interaction occurred between each of the LAs in binary mixtures with myristic acid, the spectrum of the binary mixture of each LA + myristic acid was compared with a mathematical addition of the individual LA + myristic acid spectra at the same eutectic ratio as the binary mixture. The overall spectrum of each LA and myristic acid was scaled to the same area before the spectral addition. The spectrum of the binary mixture was then scaled to the same area as that of the spectral addition to allow comparison of relative band intensities. The band assignments for both LAs and myristic acid are given in Table 1.

Spectra of the binary mixture at the eutectic ratio and the calculated spectral addition of bupivacaine– and ropivacaine–myristic acid at the eutectic ratio are presented in Fig. 2A and B, respectively. In the absence of any interaction between myristic acid and LA in the binary mixture, the calculated 1 : 1 spectral addition (ii) should have very similar relative intensities and band positions as the 1 : 1 binary mixture in (iii). However, distinct differences in the relative intensities of several bands were evident indicating some degree of interaction of each LA with myristic acid. The most prominent

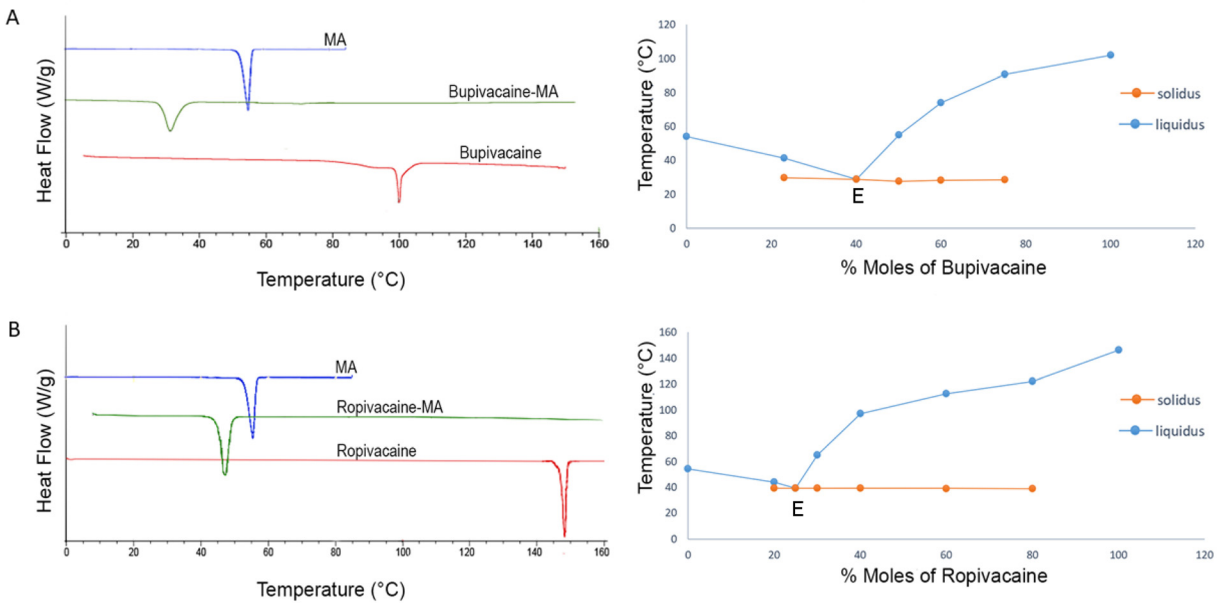

Fig. 1 DSC thermograms (left) and phase diagrams (right) of A. bupivacaine–myristic acid and B. ropivacaine–myristic acid binary mixtures. The point, E, where the liquidus curves and solidus intersect, is termed the eutectic point.

Table 1 Band assignments for the functional groups in the spectra of lidocaine, bupivacaine and ropivacaine

Band	Band assignment
687 cm^{-1}	C–O in-plane deformations[28]
707 cm^{-1}	HNC twisting and wagging, C–O out of plane deformations[25,28,29]
720 cm^{-1}	Ring torsion, ring-CH wagging, C–O out of plane deformations[25,28,29]
732 cm^{-1}	HNC twisting and wagging, C–O out of plane deformations[25]
753 cm^{-1}	Ring torsion, ring-CH wagging, C–O out of plane deformations[25,28]
768 cm^{-1}	Ring torsion, ring-CH wagging, HNC wagging[25]
813 cm^{-1}	CH_3 rocking, CH_2 rocking and ν_s NC_2 stretching[25]
941 cm^{-1}	C–O–C and O–H deformations of carboxylic acids[25]
952(sh) cm^{-1}	C–C stretching, NCO scissoring[25,28]
968 cm^{-1}	Aromatic ring –C–H wagging[25]
985 cm^{-1}	CH_2 rocking and ring –C–H wagging[25]
1003 cm^{-1}	CH_2 rocking and ring –C–H wagging[25]
1035 cm^{-1}	$\delta(CH_3)$ C–H rocking[25]
1074 cm^{-1}	$\delta(CH_3)$ C–H rocking[25,28]
1094 cm^{-1}	CH_2 twisting, CH_3 rocking and NC_2 twisting[25]
1124 cm^{-1}	–C–H in plane bend, ring stretching and breathing[25]
1169cm^{-1}	C–N stretching, CH_2 rocking[25]
1190 cm^{-1}	C–O, C–C stretching, C–O–H, C–O–C deformations[25]
1209 cm^{-1}	Amide III C–C stretching, ring bending and HNC scissor[25]
1212 cm^{-1}	Amide III C–C stretching, ring bending and HNC scissor[25]
1237 cm^{-1}	Amide III C–C stretching, ring bending and HNC scissor[25]
1262 cm^{-1}	Amide III C–C stretching, ring bending and HNC scissor[25]
1296 cm^{-1}	$\gamma(CH_2)$ twisting[25]
1307 cm^{-1}	C–N stretch, $\gamma(CH_2)$ twisting[25]
1328 cm^{-1}	C–N stretch, $\gamma(CH_2)$ deformations[25]
1369 cm^{-1}	$\gamma(CH_2)$ twisting and wagging[25]
1383 cm^{-1}	$\gamma(CH_2)$ wag and $\delta(CH_3)$ deformations[25]
1410 cm^{-1}	C–N stretch[25,28]
1448 cm^{-1}	$\delta_{as}(CH_3)$ and ring C–H in plane bend and deformations, O–H deformation modes[25,27,30]
1472 cm^{-1}	$\delta(CH_2)$ C–H deformations and O–H deformation modes[25,27,30]
1498 cm^{-1}	$\delta_{as}(CH_3)$ and $\delta(CH_2)$ C–H deformations[25]
1550 cm^{-1}	δ(C═N–H) and ν(N–C)[29]
1595 cm^{-1}	δ(C═N–H) and ν(N–C)[25]
1668 cm^{-1}	δ(C═N–H) and ν(N–C═O)[25,29]
1688 cm^{-1}	>C═O stretching of carboxylic acid[25,29]
1701 cm^{-1}	>C═O stretching of carboxylic acid[25,29]
2500–2700 cm^{-1}	O–H stretching vibrations of carboxylic acid dimers[27]
2805 cm^{-1}	$\nu_{as}(CH_2)$ and $\nu_s(CH_2)$ C–H stretching[25]
2847 cm^{-1}	$\nu_s(CH_2)$[25]
2857 cm^{-1}	$\nu_s(CH_2)$[25]
2874 cm^{-1}	$\nu_s(CH_3)$[25]
2920 cm^{-1}	C–H stretching (asym) of $>CH_2$ in fatty acids[25]
2928 cm^{-1}	$\nu_{as}(CH_2)$ and $\nu_s(CH_2)$ C–H stretching[25]
2955 cm^{-1}	C–H stretching (asym) of $-CH_3$ [25]
2960 cm^{-1}	C–H stretching (asym) of $-CH_3$ [25]
2972 cm^{-1}	$\nu_{as}(CH_2)$, $\nu_{as}(CH_3)$ & $\nu_s(CH_3)$ C–H stretching[25]
3003 cm^{-1}	$\nu_{as}(CH_3)$[25]
3115 cm^{-1}	$\nu_{as}(CH_3)$[25]
3157 cm^{-1}	$\nu_{as}(CH_3)$[25]
3170 cm^{-1}	$\nu_{as}(CH_3)$[25]
3252 cm^{-1}	N–H stretching and ν_{as} (–CH) stretching[25,29,31]
3432 cm^{-1}	N–H stretching of (H–N–C═O) amide[25,31]
3448 cm^{-1}	ν(N–H) free $-NH$[25,31]

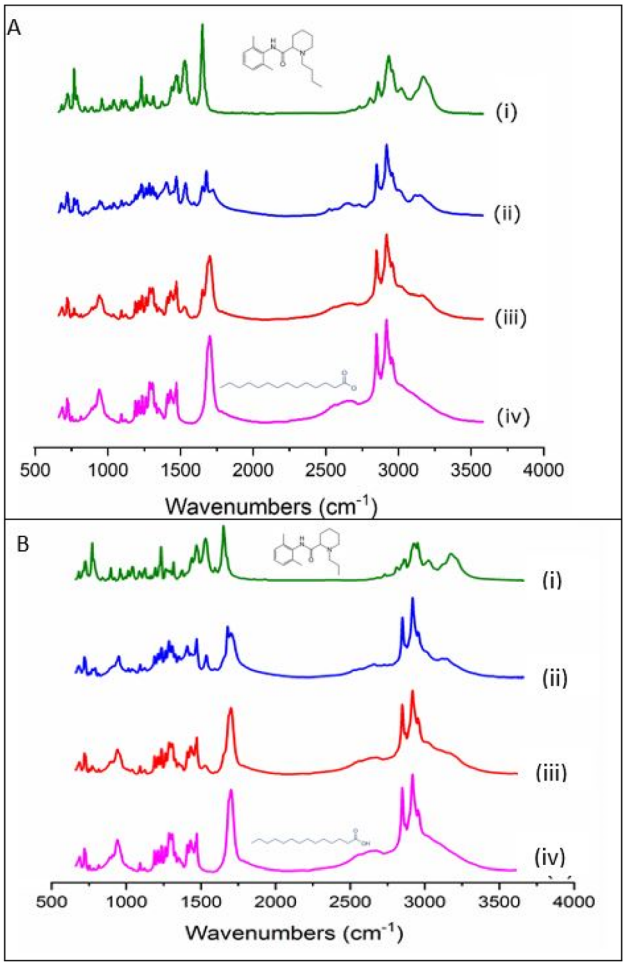

Fig. 2 Comparison of the FTIR spectra of A. (i) bupivacaine, (ii) bupivacaine–myristic acid eutectic mixture (2 : 3), (iii) bupivacaine–myristic acid (2 : 3) spectral addition, and (iv) myristic acid, and B. (i) ropivacaine, (ii) ropivacaine–myristic acid eutectic mixture (1 : 3), (iii) ropivacaine–myristic acid (1 : 3) spectral addition, and (iv) myristic acid.

difference was observed in the C═O stretching mode of myristic acid, which is represented in the pure form by a strong peak at 1701 cm^{-1} with a shoulder at 1686 cm^{-1}. This split in frequency is believed to be due to different conformations of the C═O group, which in the condensed phase of myristic acid occurs predominantly in the form of hydrogen bonded dimers.[27] As previously observed in binary mixtures of lidocaine and myristic acid,[20] a loss in intensity of this myristic acid C═O band was observed in the binary mixtures with bupivacaine and ropivacaine in comparison to their respective mathematically added spectra (iii). However, in the lower fingerprint region and in the C–H and N–H stretching regions, both bupivacaine (Fig. 3A) and ropivacaine (Fig. 3B) responded differently from lidocaine in binary mixtures with myristic acid. Similar changes were observed in the spectra for bupivacaine and ropivacaine when in binary mixtures with myristic acid, indicating similar interactions of these two drugs with the myristic acid.

In the bupivacaine–myristic acid binary mixtures, the myristic acid C═O stretch shifts from 1701 to 1723 cm^{-1}

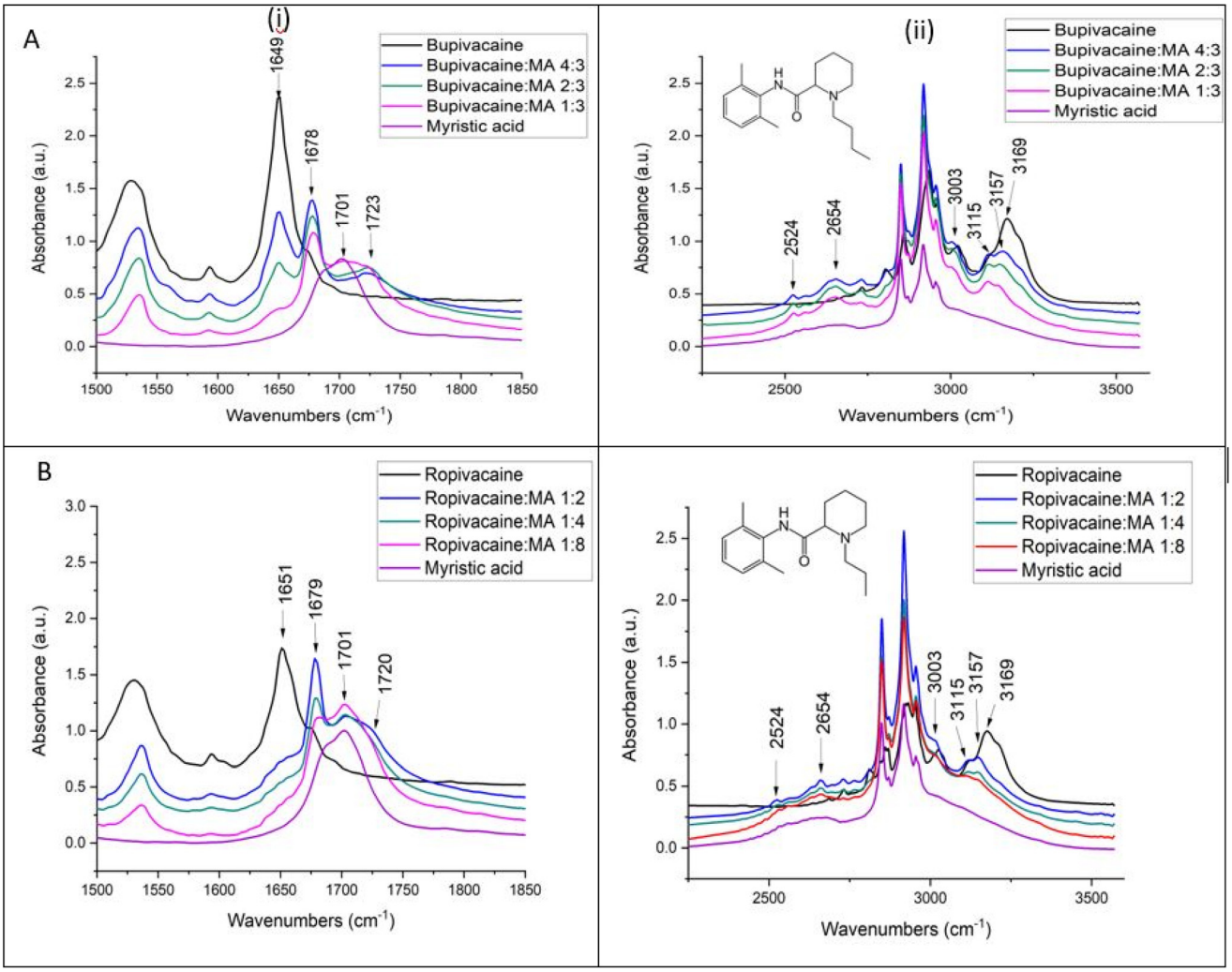

Fig. 3 Spectra in overlaid format, slightly offset for clarity, of myristic acid (MA) and its binary mixtures with A. bupivacaine and B. ropivacaine (i) in the amide 1 band region and (ii) in the C–H and N–H stretching region.

accompanied by a shift in the amide 1 C═O stretching of bupivacaine to 1678 cm^{-1}. At the same time, the broad bands of myristic acid between 2500 and 2800 cm^{-1} resolve into sharper and more distinct bands at 2524, 2558, 2624 and 2654 cm^{-1}. The broadness of the bands in this region is typical for the O–H stretching modes of carboxylic acids and explained by hydrogen bonding with some dimer formation.[27,30,32] The increased resolution of this broad band into distinct bands in the binary mixtures with bupivacaine can be explained by more defined O–H stretching frequencies of the myristic acid O–H groups, due to hydrogen bonding with the C═O groups of bupivacaine, as suggested by a red-shift of the bupivacaine C═O amide 1 band. Furthermore, some hydrogen bonding between myristic acid O–H and the slightly negatively charged N lone pair sites on the piperidine ring is also likely.[33] Similar observations were made for the ropivacaine–myristic acid binary mixtures in Fig. 3B. In contrast to lidocaine–myristic acid binary mixtures reported previously,[20] no evidence of a shift to higher frequencies of the N–H stretching mode was observed in binary mixtures of either bupivacaine or ropivacaine. Instead, the aromatic ring 3169 cm^{-1} C–H stretching mode of both the LAs shifts to a lower frequency (3157 cm^{-1}) with changes in the relative intensity of this band and the other aromatic C–H stretching mode at 3115 cm^{-1}.

Two-dimensional correlation Fourier-transform infrared spectroscopy (2DCOS FTIR)[24] was performed to further analyse the interactions occurring as increasing amounts of myristic acid were added to each LA in the binary mixtures. In particular, the synchronous 2D correlation plots provided an overview of which vibrational modes of each LA and myristic acid underwent change simultaneously as the ratio of myristic acid in their binary mixtures was increased. The autopeaks in the synchronous 2D correlation map lie along the diagonal line and are always red (non-negative); these identify the biggest spectral intensity changes occurring in the set of binary mixtures. The cross peaks located on either side of the diagonal show correlations between peak changes at two different spec-

tral values: v1 (horizontal axis spectrum) and v2 (vertical axis spectrum). Red cross peaks measured at v1 and v2 in the synchronous 2D correlation map represent those peak intensities that are changing in the same direction, *i.e.*, the intensities of both are either increasing or decreasing simultaneously with the perturbation, which for each of the bupivacaine/myristic acid and ropivacaine/myristic acid binary mixtures, is the increasing ratio of myristic acid added to each LA. The blue cross peaks show which peak intensities measured at v1 and v2 are changing in opposite directions, *i.e.*, one increasing while the other is simultaneously decreasing with the perturbation. The 2D COS synchronous maps for bupivacaine- and ropivacaine–myristic acid binary mixtures are given in Fig. 4A and B, respectively.

The autopeaks at 2917 cm^{-1} and 1701 cm^{-1} are identified as the peaks undergoing the biggest intensity change in this binary mixture set; these are for myristic acid. The red and blue cross peaks for bupivacaine (Fig. 4A) and ropivacaine (Fig. 4B) are very similar; this shows similar interactions occurring between myristic acid and each of these LAs as the myristic acid content is increased.

For each of the bupivacaine and ropivacaine binary mixtures with myristic acid, blue cross peaks for pairs **M′N′** represent a decrease in the LA 1530 cm^{-1} (aromatic ring C–H deformations) and a decrease in amide 1 C═O 1649 cm^{-1} stretching as the 2849 cm^{-1} (C–H stretching) of myristic acid increases. This coincides with the red cross peaks at **M′N′** that represent an increase in hydrogen bonded amide 1 C═O band at 1676 cm^{-1} with increasing C–H stretching myristic acid bands at 2948 and 2955 cm^{-1}. The blue cross peaks at **U′V′** show that there is a decrease in both the amide 1 C═O at 1649 cm^{-1} and aromatic ring C–H stretching at 1530 cm^{-1}, as hydrogen bonding occurs on the amide 1 C═O at 1676 cm^{-1} with increasing myristic acid. The red cross peaks at **U′V′** show the simultaneous decrease in the relative intensities of the aromatic ring C–H deformations of bupivacaine and ropivacaine bands at 1530 cm^{-1} and the amide 1 C═O 1649 cm^{-1} as increasing levels of myristic acid are added to the binary mixtures.

The red cross peaks at **O′P′** show decrease in the 1289 cm^{-1} CH_2 deformations with loss of the myristic acid 1701 cm^{-1} C═O stretching band, suggesting that hydrogen bonding of the myristic acid C═O occurs with the C–H of ethyl groups on bupivacaine and ropivacaine. Also, the red cross peaks near **Q′R′** show the simultaneous decrease in the myristic acid 937 cm^{-1} O–H deformation as it shifts to 957 cm^{-1}, with decrease in the 1701 cm^{-1} C═O stretching as it shifts to 1723 cm^{-1}; these shifts result from hydrogen bonding between the myristic acid O–H and the bupivacaine and ropivacaine amide 1 C═O.

The asynchronous 2D cos plots for bupivacaine and ropivacaine are shown in Fig. 5A and B, respectively. These maps demonstrate the direction in which the spectral intensities vary with increasing myristic acid ratio, with the cross peaks indicating those band intensities that are changing sequentially or out-of-phase, *i.e.*, not simultaneously with increases in

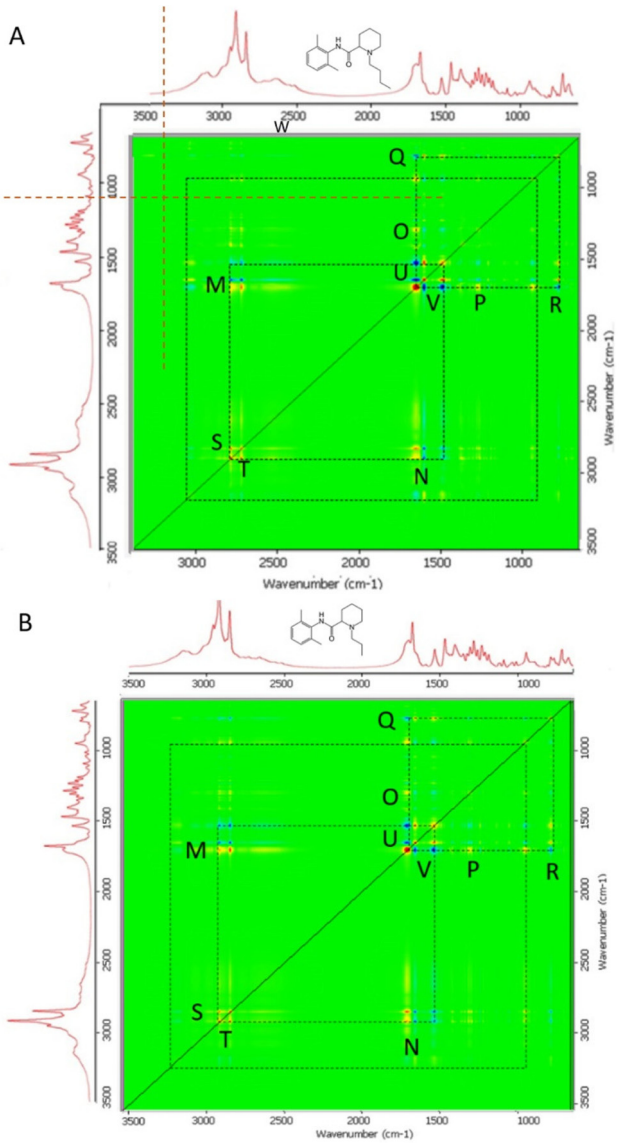

Fig. 4 Synchronous 2D correlation maps for the spectra of binary mixtures of A. bupivacaine and B. ropivacaine with myristic acid. Correlations between the spectra are monitored for five different LA and myristic acid mixtures: the LA alone, three binary mixtures with increasing ratio of myristic acid, and myristic acid alone and their average was used as the reference spectra. Autopeaks occur along the diagonal line; the main cross peaks are labelled.

myristic acid levels. The cross peaks changes are unsynchronized and represent contributions from individual functional groups experiencing different effects as the levels of MA are increased. This could indicate different molecular environments experienced by one of the functional groups than those experienced by the other parts of the molecule, as increasing levels of MA are added. The closely spaced peaks can indicate overlapping bands in which one of the components changes while other do not. The presence of cross peaks in each plot shows evidence of specific interactions between myristic acid and each LA: for purely non-interacting binary mixtures, there

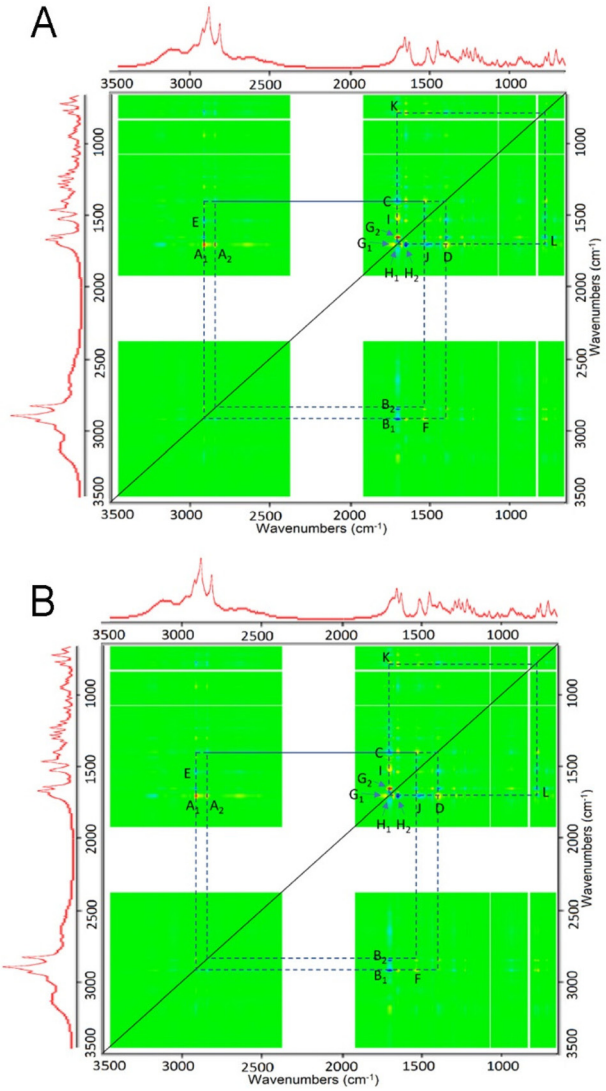

Fig. 5 Asynchronous 2D correlation maps for the spectra of binary mixtures of A. bupivacaine and B. ropivacaine with myristic acid. Correlations between the spectra are monitored for five different LA and myristic acid mixtures: the LA alone, three binary mixtures with increasing ratio of myristic acid, and myristic acid alone. Their average was used as the reference spectrum. The main cross peaks are labelled.

will be no asynchronous cross peaks. The red cross peaks indicate the peaks in v1 (the horizontal axis) that undergo spectral intensity changes before, or to a greater extent than the peaks in v2 (vertical axis) as myristic acid levels increase in each binary mixture. The blue cross peaks indicate the peaks in v2 that undergo intensity changes before or to a greater extent than the peaks in v1.[34]

A cluster of four cross peaks of opposing signs located on opposite sides of the diagonal are seen at C′D′I′J′ on the top right section between 1300 and 1800 cm^{-1}. These represent peaks undergoing a shift in position (Noda and Ozaki, 2004). Red cross peaks I′ and D′ appear at 1701 (ν_1) & 1526 (ν_2) cm^{-1}, and 1399 and 1704 cm^{-1}, respectively. These correspond with the blue cross peaks C′ at 1701 & 1501 cm^{-1} and J′ at 1526 & 1701 cm^{-1}, respectively. These bands are characteristic for the amide II δ(C–N–H) and ν(N–C) and myristic acid C=O stretching modes, which undergo shift due to changes in hydrogen bonding as myristic acid is added. Also, closely spaced red cross peaks appear at G2′ (1701 (ν_1) & 1656 (ν_2) cm^{-1}) and G1′ (1730 & 1701 cm^{-1}) that correspond with blue cross peaks at H1′ (1701 & 1730 cm^{-1}) and H2′ (1656 & 1701 cm^{-1}). These indicate different extents of interaction between the C=O stretching modes of myristic acid (1701 and 1730 cm^{-1}) and the amide I C=O stretching modes for bupivacaine and ropivacaine (1656 cm^{-1}) as increasing levels of MA are added to the binary mixtures.

Additional cross peaks are seen in the bottom right and top left quadrants of the asymmetric plots in Fig. 5. Red cross peaks appear at A_1′ (2921 (ν_1) & 1701 (ν_2) cm^{-1}) and A_2 ·(2852 & 1701 cm^{-1}), and F′ (1541 & 2921 cm^{-1}), while the corresponding blue cross peaks appear at B_1′ (1701 & 2921 cm^{-1}), B_2′ (1701 & 2852 cm^{-1}) and E′ (2921 & 1541 cm^{-1}), respectively. The opposite signs of F′ and E′, and A_1′, A_2′ and B_1′B_2′ indicate that upon formation of the binary mixtures and with increasing levels of MA, the amide I and II bands of the LAs at 1541 cm^{-1} and both the C=O stretching mode at 1701 cm^{-1} and C–H stretching bands at 2852 and 2921 cm^{-1} of MA, undergo band shifts due to changes in hydrogen bonding within each LA and between the LAs and myristic acid.

The red and blue cross peaks described above in the asymmetric plots of each of the bupivacaine and ropivacaine binary mixtures with MA further confirm the hypothesis that the intermolecular hydrogen bonding within each LA is reduced or lost in the binary mixture. The myristic acid monomers, resulting from loss of the hydrogen bonded dimers, form hydrogen bonds with the LAs, mainly between the C=O group of the LA amide and the C=O of myristic acid, but also between the LA –C=O and myristic acid –O–H. It may be hypothesized that the stronger pull of electrons by the aromatic ring and the C=O of the amide group in each LA results in a slightly positive O–H environment which becomes susceptible to hydrogen bonding with the C=O of myristic acid.[25,26]

The above observations indicate hydrogen bonding interaction between myristic acid and both, bupivacaine and ropivacaine. Although no increased frequency shift for the N–H stretch mode was observed at the eutectic ratio, a significant reduction in intensity of the 3116 cm^{-1}, 3170 cm^{-1} and 3205 cm^{-1} modes with a small red shift for 3170 cm^{-1} mode was noted. These bands contain contributions from both O–H stretching of myristic acid dimers and C–H stretching modes of the aromatic ring. The simultaneous increased definition of the O–H stretching modes of the myristic acid dimer structures between 2500 and 2800 cm^{-1} are probably associated with hydrogen bonding of the myristic acid O–H groups with the bupivacaine and ropivacaine amide C=O. Previous FTIR studies evaluating complexation of bupivacaine and ropivacaine with cyclodextrins have also observed a carbonyl peak at 1678 cm^{-1}, believed to be due to a reduction in crystallinity of the LA molecules.[35,36] In the present study, the new amide 1 C=O peak observed at 1678 and 1679 cm^{-1} in myristic acid

binary mixtures with bupivacaine and ropivacaine, respectively, is proposed to be due to the LA C═O group forming hydrogen bonds with the myristic acid –O–H. This is supported by the simultaneous shift of the myristic acid O–H deformation modes at 939 cm^{-1} to 956 cm^{-1}. This in turn leads to reduced interaction between adjacent LA molecules, reducing crystallization. In the ropivacaine binary mixtures with myristic acid, the secondary amide C–N stretch and C–N–H in plane bend at 1535–1546 cm^{-1} (ref. 37 and 38) also seemed to become sharper, suggesting a more ordered structure for the ropivacaine binary mixture with MA than within ropivacaine alone. Moreover, while the ropivacaine and myristic acid eutectic formation was observed only when three moles of myristic acid were present for every mole of ropivacaine, the residual 1701 cm^{-1} band in the binary mixtures suggests that the excess myristic acid in these mixtures does not participate in hydrogen bonding with ropivacaine, but likely inhibits interaction between adjacent ropivacaine molecules by steric hindrance. Also, for the bupivacaine : myristic acid binary mixtures, the residual 1701 cm^{-1} band was obvious only in the 1 : 3 mixture but not at the eutectic ratio of 2 : 3. These observations suggest that hydrogen bonding interaction between bupivacaine and myristic acid is more favourable than that between ropivacaine and myristic acid.

This mechanism of this interaction of bupivacaine and ropivacaine with myristic acid differs considerably from that we previously observed between lidocaine and myristic acid,[20] possibly due to change the symmetry of the molecule by the piperidine ring of bupivacaine and ropivacaine in which the N lone pair may and attract H-bonding with myristic acid.

Crystallisation in EVA films containing local anaesthetic and myristic acid

The EVA films were visually evaluated for opacity and crystallization over time. Relatively higher drug loading could be achieved with bupivacaine than with ropivacaine. As shown in Table 2, crystallization of both bupivacaine and ropivacaine was impeded by myristic acid at the 1-week and 1-month timepoints. However, by the 6-month timepoint, crystallization was observed in all EVA films, except those containing 3% w/w bupivacaine, alone or in combination with myristic acid.

Our previous studies have suggested that eutectic formation between lidocaine and myristic acid inhibits lidocaine crystallization in EVA by reducing molecular interaction between adjacent lidocaine molecules.[20] In the present study, addition of myristic acid only transiently inhibited the crystallization of bupivacaine and ropivacaine, suggesting that intermolecular interactions between adjacent molecules of bupivacaine and ropivacaine, respectively, were stronger than those formed by hydrogen bonding with myristic acid. Previously, Gala *et al.*[39] have suggested that compounds having similar melting and recrystallization temperatures with high intermolecular hydrogen bonding capability form more stable eutectics that are least likely to crystallize. Meanwhile, when crystallization peaks of eutectic components do not lie close to each other, then their eutectic mixture is likely to crystallize readily. This explains the strong interaction we have previously observed between lidocaine and myristic acid, both of which have similar melting and recrystallization temperatures.[20] Meanwhile, the melting temperature of myristic acid differs significantly from that of bupivacaine and ropivacaine. Therefore, it is likely that as the mixture achieves thermodynamic equilibrium, the pure components recrystallize separately at their respective temperatures, disrupting hydrogen bonding interaction and rendering the system unstable; thus, eventually leading to crystallization of both bupivacaine and ropivacaine in EVA even in the presence of myristic acid by the 6-month timepoint.

Table 2 Visual observation of EVA films over 6 months

LA concentration (% w/w)	LA : myristic acid molar ratio	Observation		
		1 week	1 month	6 months
Bupivacaine 3%	No myristic acid	Clear	Clear	Clear
Bupivacaine 3%	1 : 1.5	Clear	Clear	Clear
Bupivacaine 6%	No myristic acid	Clear	Crystals	Crystals
Bupivacaine 6%	1 : 1.5	Clear	Clear	Crystals
Bupivacaine 9%	No myristic acid	Crystals	Crystals	Crystals
Bupivacaine 9%	1 : 1.5	Clear	Crystals	Crystals
Ropivacaine 3%	No myristic acid	Crystals	Crystals	Crystals
Ropivacaine 3%	1 : 3	Clear	Clear	Crystals
Ropivacaine 6%	No myristic acid	Crystals	Crystals	Crystals
Ropivacaine 6%	1 : 3	Clear	Crystals	Crystals
Ropivacaine 9%	No myristic acid	Crystals	Crystals	Crystals
Ropivacaine 9%	1 : 3	Crystals	Crystals	Crystals

Conclusion

The present study suggests that myristic acid binary mixtures with bupivacaine and ropivacaine form a eutectic at the ratio of 2 : 3 and 1 : 3, respectively, due to hydrogen bonding interactions between myristic acid C═O and O–H groups with the bupivacaine and ropivacaine amide C═O. For both drugs, the thermodynamic eutectic ratio is observed when myristic acid is present in excess in the binary mixtures, although spectroscopic studies suggest that not all myristic acid molecules are engaged in the hydrogen bonding interaction. Furthermore, in contrast to our previous observations in lidocaine and myristic acid binary mixtures, the NH-mode of the amide group of bupivacaine and ropivacaine is not involved in hydrogen bonding interactions with myristic acid, likely due to change in the symmetry of the molecule by the piperidine ring of bupivacaine and ropivacaine. Overall, the eutectic mixture of bupivacaine and ropivacaine appears to inhibit bupivacaine and ropivacaine crystallization in EVA only transiently.

Author contributions

P. A. – conceptualization, data curation, formal analysis, investigation, writing – original draft; D. S. – conceptualization, project administration, funding acquisition, resources, writing –

review and editing; M. N. – conceptualization, methodology, data curation, validation, writing – original draft.

Conflicts of interest

There are no conflicts to declare.

References

1 W. S. MacFater, W. Xia, A. Barazanchi, B. Su'a, D. Svirskis and A. G. Hill, *World J. Surg.*, 2018, **42**, 3112–3119.
2 N. Eipe, S. Gupta and J. Penning, *BJA Educ.*, 2016, **16**, 292–298.
3 W. S. MacFater, W. Xia, A. W. H. Barazanchi, N. J. Lightfoot, M. Weston, D. Svirskis and A. G. Hill, *Ann. Surg.*, 2022, **275**, e30–e36.
4 R. S. Sinatra, J. S. Jahr and J. M. Watkins-Pitchford, *The Essence of Analgesia and Analgesics*, Cambridge University Press, Cambridge, 1st edn, 2010.
5 C. W. Clarkson and L. M. Hondeghem, *Anesthesiology*, 1985, **62**, 396–405.
6 C. R. Cox, K. A. Faccenda, C. Gilhooly, J. Bannister, N. B. Scott and L. M. Morrison, *Br. J. Anaesth.*, 1998, **80**, 289–293.
7 C. M. Brummett, M. A. Norat, J. M. Palmisano and R. Lydic, *Anesthesiology*, 2008, **109**, 502–511.
8 K. L. Thornton, M. D. Sacks, R. Hall and R. Bingham, *Paediatr. Anaesth.*, 2003, **13**, 409–412.
9 A. Kaur, R. B. Singh, R. K. Tripathi and S. Choubey, *J. Clin. Diagn. Res.*, 2015, **9**, UC01–UC06.
10 D. B. Scott, A. Lee, D. Fagan, G. M. Bowler, P. Bloomfield and R. Lundh, *Anesth. Analg.*, 1989, **69**, 563–569.
11 A. Casati and M. Putzu, *Best Pract. Res., Clin. Anaesthesiol.*, 2005, **19**, 247–268.
12 S. L. Brown and A. E. Morrison, *Anesthesiology*, 2004, **100**, 1305–1307.
13 A. Koogler, G. Amusa, M. Kushelev, A. Lawrence, L. Carlson and K. Moran, *SAGE Open Med. Case Rep.*, 2019, **7**.
14 C. L. Jeng, T. M. Torrillo and M. A. Rosenblatt, *Br. J. Anaesth.*, 2010, **105**(Suppl 1), i97–107.
15 A. Swain, D. S. Nag, S. Sahu and D. P. Samaddar, *World J. Clin. Cases*, 2017, **5**, 307–323.
16 A. L. Balocco, P. G. E. Van Zundert, S. S. Gan, T. J. Gan and A. Hadzic, *Curr. Opin. Anesthesiol.*, 2018, **31**, 636–642.
17 T.-F. Li, H. Fan and Y.-X. Wang, *PLoS One*, 2015, **10**, e0117321–e0117321.
18 A. Hadzic, H. S. Minkowitz, T. I. Melson, R. Berkowitz, A. Uskova, F. Ringold, J. Lookabaugh and B. M. Ilfeld, *Anesthesiology*, 2016, **124**, 1372–1383.
19 D. Svirskis, G. Procter, M. Sharma, P. Bhusal, A. Dravid, W. MacFater, A. Barazanchi, L. Bennet, K. Chandramouli, S. Sreebhavan, P. Agarwal, S. Amirapu, J. A. Hannam, G. P. Andrews, A. Hill and D. S. Jones, *Biomaterials*, 2020, **263**, 120409.
20 P. Agarwal, M. K. Nieuwoudt, S. Li, G. Procter, G. P. Andrews, D. S. Jones and D. Svirskis, *Int. J. Pharm.*, 2022, **621**, 121819.
21 Z.-R. Liu, Y.-H. Shao, C.-M. Yin and Y.-H. Kong, *Thermochim. Acta*, 1995, **250**, 65–76.
22 P. Bhusal, M. Sharma, J. Harrison, G. Procter, G. Andrews, D. S. Jones, A. G. Hill and D. Svirskis, *J. Chromatogr. Sci.*, 2017, **55**, 832–838.
23 S. G. Avula, K. Alexander and A. Riga, *J. Therm. Anal. Calorim.*, 2010, **99**, 655–658.
24 D. Law, W. Wang, E. A. Schmitt and M. A. Long, *Pharm. Res.*, 2002, **19**, 315–321.
25 H. M. Badawi, W. Förner and S. A. Ali, *Spectrochim. Acta, Part A*, 2015, **142**, 382–391.
26 H. M. Badawi, W. Förner and S. A. Ali, *Spectrochim. Acta, Part A*, 2016, **152**, 92–100.
27 B. L. Van Hoozen and P. B. Petersen, *J. Chem. Phys.*, 2015, **142**, 104308.
28 G. Socrates, *J. Am. Chem. Soc.*, 2002, **124**, 1830–1830.
29 M. L. Martins, J. Eckert, H. Jacobsen, E. C. dos Santos, R. Ignazzi, D. R. de Araujo, M.-C. Bellissent-Funel, F. Natali, M. Marek Koza, A. Matic, E. de Paula and H. N. Bordallo, *Data Brief*, 2017, **15**, 25–29.
30 B. L. Van Hoozen Jr. and P. B. Petersen, *J. Chem. Phys.*, 2017, **147**, 224304.
31 V. K. Ramiah and P. G. Puranik, *Proc. – Indian Acad. Sci. Sect. A*, 1962, **56**, 96–102.
32 I. Tsivintzelis, G. M. Kontogeorgis and C. Panayiotou, *J. Phys. Chem.*, 2017, **121**, 2153–2163.
33 C. E. Lobato-García, P. Guadarrama, C. Lozada, R. G. Enríquez, D. Gnecco and W. F. Reynolds, *J. Mol. Struct.*, 2006, **786**, 53.
34 I. Noda, *Appl. Spectrosc.*, 1993, **47**, 1329–1336.
35 M. Jug, F. Maestrelli, M. Bragagni and P. Mura, *J. Pharm. Biomed. Anal.*, 2010, **52**, 9–18.
36 G. Dollo, P. Le Corre, F. Chevanne and R. Le Verge, *Int. J. Pharm.*, 1996, **131**, 219–228.
37 E. Goormaghtigh, V. Cabiaux and J. M. Ruysschaert, *Subcell. Biochem.*, 1994, **23**, 363–403.
38 V. Niederwanger, F. Gozzo and U. J. Griesser, *J. Pharm. Sci.*, 2009, **98**, 1064–1074.
39 U. Gala, M. C. Chuong, R. Varanasi and H. Chauhan, *AAPS PharmSciTech*, 2015, **16**, 528–536.